



Investigating the impact of thermal annealing on the photovoltaic performance of chemical bath deposited SnO₂/p-Si heterojunction solar cells

Anannya Bhattacharya¹ · Jenifar Sultana² · Subhrajit Sikdar¹ · Rajib Saha¹ · Sanatan Chattopadhyay¹

Received: 15 October 2019 / Accepted: 20 October 2019 / Published online: 31 October 2019
© Springer-Verlag GmbH Germany, part of Springer Nature 2019

Abstract

The current work investigates the impact of annealing temperature on the optoelectronic properties of SnO₂ thin films grown by chemical bath deposition (CBD) method. The as-grown SnO₂ films, on p-Si substrate, are annealed at 200 °C and 400 °C for 10 min in Ar ambient for investigating the impact of such annealing on the performance of SnO₂/p-Si heterojunction solar cells. The growth of a uniform SnO₂ film on Si surface has been confirmed from SEM studies and the chemical composition and optical properties of the as-grown and annealed films are investigated in detail by employing XRD and ellipsometric measurements. Absorption coefficient of the samples is observed to vary in the range of $24 \times 10^5 - 60 \times 10^5/\text{m}$, at its band gap (3.0 eV). The current–voltage characteristics under both dark and illuminated conditions suggest superior voltaic performance of the 200 °C annealed SnO₂ film. The short-circuit current density, open-circuit voltage and fill-factor are obtained to be 0.45 mA/cm², 5.41 mA/cm² and 0.4 V, 0.34 V and 13%, 8% respectively for as-grown and 200 °C annealed samples. The maximum power conservation efficiency (η) of 4.9% is obtained for the 200 °C annealed sample. Thus, the study indicates the potential of CBD-grown SnO₂ film for photovoltaic applications.

1 Introduction

The metal-oxide semiconductors such as zinc oxide (ZnO), tin oxide (SnO₂), copper oxide (CuO), indium oxide (In₂O₃), tungsten trioxide (WO₃) and titanium dioxide (TiO₂) are gaining significant research interests in the domain of electronics and opto-electronics for their unique and tunable material, chemical, electrical and optical

properties. Moreover, the low-cost, non-toxicity and natural abundance have been emerged to be the governing factors for the design and development of thin film or nanostructure based metal-oxide devices for several applications including photovoltaics (Yu et al. 2016; Block and Schmäcker 2016; Comini et al. 2002; Baby and Ramaprabhu 2012; Pérez-Tomás et al. 2017).

Among various metal-oxides, SnO₂ has gained significant research and commercial interest owing to its promising electro-optical properties, excellent chemical and physical stability. Stannum (Sn) is a post-transition metal with variable oxidation states 2 and 4, and therefore can form two type of oxides, stannous oxide (SnO) and stannic oxide (SnO₂). The nature of SnO₂ can be either n- or p-type semiconductor, depending upon its oxygen defects (Bendjedidi et al. 2015; Bae et al. 2017). Its relatively higher electron mobility (106 cm²/V s with a carrier density of $3.0 \times 10^{18}/\text{cm}^3$) (Mun et al. 2015), low sheet resistance, superior light transmittance (Tripathy et al. 2013), low chemical and photo-catalytic reactivity (Liu et al. 2016) and easy synthesis technique at room temperature (Tazikeh et al. 2014) are useful for developing different semiconductor devices. Also, the high band gap of SnO₂ in the range of 3.0–3.7 eV (Xiong et al. 2018) makes

✉ Sanatan Chattopadhyay
scelc@caluniv.ac.in

Anannya Bhattacharya
anannyabh13@gmail.com

Jenifar Sultana
sultanajenifar@gmail.com

Subhrajit Sikdar
subhrajit.sikdar@yahoo.com

Rajib Saha
saharajib836@gmail.com

¹ Department of Electronic Science, University of Calcutta, Calcutta 700009, India

² Centre for Research in Nanoscience and Nanotechnology (CRNN), University of Calcutta, Calcutta 700098, India

it potentially a superior material for window layer in solar cells (Xiong et al. 2018; Zhou et al. 2018).

Several methods such as atomic layer deposition (ALD) (Cheng et al. 2012), sputtering (Leng et al. 2012), thermal evaporation (Patel et al. 2013), sol–gel (Dong et al. 2015) and spray pyrolysis (Jadsadapattarakul et al. 2008) have been attempted to grow crystalline SnO₂ thin films. However, all of these processes are either expensive with complex fabrication procedures or time consuming. In contrast, chemical bath deposition (CBD) is reported to be a controlled precipitation technique with low economical budget, simplicity and capable of large area deposition (Sultana et al. 2018). It is also possible to optimize the film morphology, thickness, grain size and crystalline quality of the grown films by precisely controlling the growth parameters and also by post-growth annealing of the grown film (Pawar et al. 2011; Mane and Lokhande 2000).

In the current work, such cost effective, low temperature (< 100 °C) CBD method is employed to grow SnO₂ thin films on Si-substrate and the impact of annealing on its morphological, optical and electrical characteristics is investigated. Surface morphology and crystallographic orientations of the SnO₂ thin films are explored by Field Emission Scanning Electron Microscopy (FESEM) and X-ray diffraction measurements respectively. The optical parameters including absorption coefficient (α) and optical band gap (E_g) have been determined by Spectroscopic ellipsometry (SE) measurements. Opto-electronic performance of the SnO₂/p-Si heterojunction diode is investigated by measuring its current–voltage (I–V) characteristics in both dark and illuminated conditions. Further, the potential of such device for photovoltaic applications is studied by extracting the values of open circuit photo-generated voltage (V_{oc}), short circuit current density (J_{sc}), fill-factor (FF) and power conversion efficiency (η) for both the as-grown and annealed samples from the relevant electrical measurements.

2 Details of CBD growth method

For the growth of SnO₂ film on p-silicon (Si) $\langle 100 \rangle$ substrate, the Si wafers were first cleaned by RCA-I and RCA-II steps and then the native oxide was removed by dipping in 20% HF solution. In the synthesis process, tin chloride dihydrate (SnCl₂·2H₂O) is used as the source of Sn²⁺ in the CBD solution and HMTA solution is used as a precursor. The bath solution was prepared by dissolving 1.128 g of SnCl₂·2H₂O in 50 ml DI water for 50 ml solution with 0.1 M strength. The solution was stirred at 180 rotations per minute (r.p.m) for 5 min. In a separate beaker, 0.1 M HMTA is added in 50 ml DI water and stirred for 5 min. These two solutions

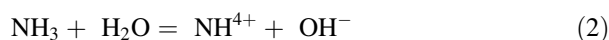
are then mixed together and stirred for 5 min at 180 rpm. The cleaned Si substrates are then placed on a Teflon holder and immersed into the solution which is under constant stirring. The beaker containing the solution is then placed on the hot plate with constant stirring and heated from room temperature to 90 °C and the growth is performed for 2 h. The post-deposition cleaning of such samples has been carried out by rinsing in DI water to remove the residual solutes and impurities and finally dried by blowing nitrogen (N₂) gas.

During the growth of SnO₂ film, HMTA in the solution bath works as a complexing agent and it primarily activates the reaction by releasing metal ions. The hydroxide ions are provided by the solvent (i.e. water). The sequential reaction mechanism for the growth of SnO₂ film by CBD method is summarized as the following:

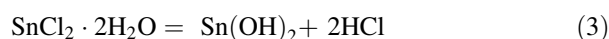
- Establishment of equilibrium between the water and complexing reagent (HMTA):



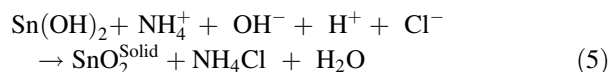
- Formation of positively charged Ammonium and negatively charged hydroxyl ion:



- Hydrolysis of the source (SnCl₂) and formation of metal ionic complexes:

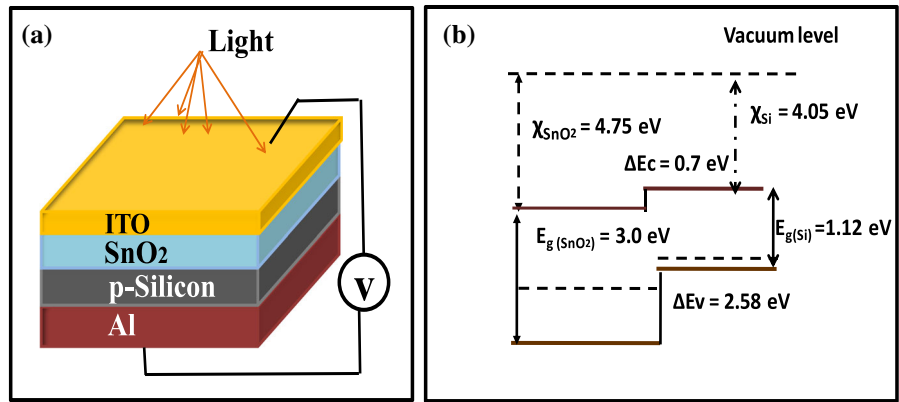


- Formation/growth of solid film on the substrate:



The grown SnO₂ film is broken into three pieces for investigating the impact of annealing on SnO₂ films. One of the samples is kept unprocessed and the rest two are thermally annealed in Argon (Ar) environment in a furnace for 10 min at 200 °C and 400 °C respectively. For having appropriate electrical contact and to measure the electrical characterization of the SnO₂/p-Si heterojunction diodes, an ITO layer of ~ 50 nm thickness is deposited on the top and Al is deposited for back contact. The device area is measured to be $1.26 \times 10^{-7} \text{ m}^2$. Considering the band gaps of p-Si and SnO₂ to be 1.12 eV and 3.0 eV respectively, the values of conduction-band offset (ΔE_c) and valence-band offset (ΔE_v) are calculated to be 0.7 eV and 2.58 eV respectively. The schematic of the fabricated device and relevant band diagram is shown in Fig. 1a, b.

Fig. 1 **a** Schematic of the fabricated SnO₂/p-Si heterojunctions devices; **b** relevant band diagram



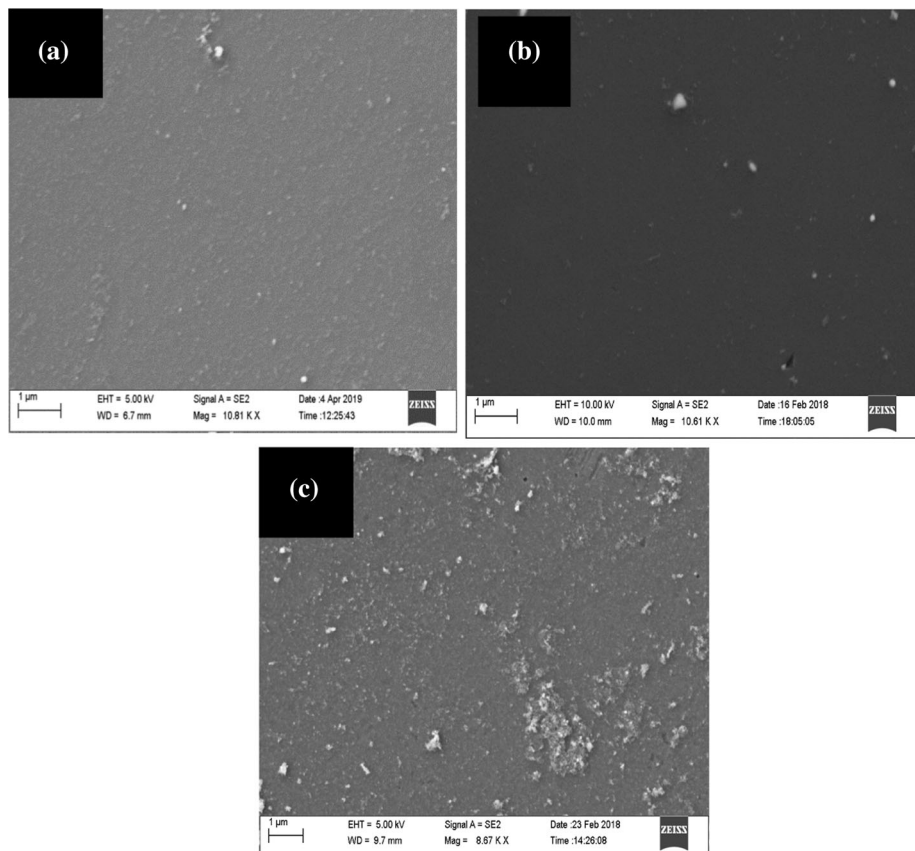
3 Results and discussion

3.1 Structural and material characterizations of SnO₂ thin film grown on p-Si substrate

Surface morphology of the as-grown, 200 °C and 400 °C annealed samples is investigated by using field-emission scanning electron microscope (ZEISS Auriga). The relevant micrographs are shown in Fig. 2a–c; respectively, which confirm the formation of a uniform film on the Si surface.

To investigate the crystallographic orientations of the grown samples, the X-ray diffraction measurements (PAN analytical X’Pert PRO XRD system) are performed and are plotted in Fig. 3. All the samples exhibit diffraction peaks that confirm the formation of rutile tetragonal structure (Chen et al. 2003) of SnO₂ thin film as verified by JCPDS card no. 77–0452. The XRD data reveal a strong diffraction peak (at $2\theta = 61.80^\circ$) corresponding to the $\langle 310 \rangle$ plane along with a peak (at $2\theta = 37.7^\circ$) corresponding to the 200) plane (Wongsaprom et al. 2014). It is an apparent from XRD data that with the increase of annealing temperature, the intensities of diffraction peaks increase and its

Fig. 2 FESEM images of the CBD grown SnO₂ thin films for the: **a** as-grown; **b** 200 °C annealed; and **c** 400 °C annealed samples



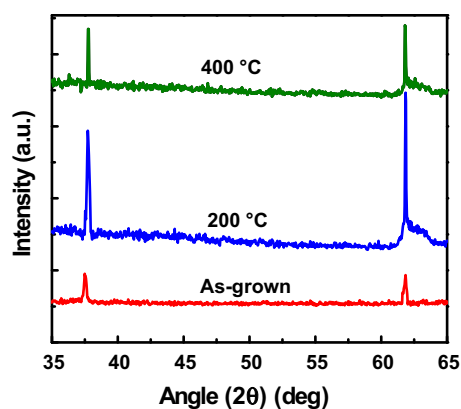


Fig. 3 Comparative plots of XRD patterns for the as-grown, 200 °C and 400 °C annealed samples

FWHM decreases. Such variation in diffraction peaks suggests an improvement of crystalline quality of the as-grown SnO₂ films upon annealing (Rasheed and Algaw 2016). The high intensity crystalline peaks at 61.8° and 37.7° for 200 °C annealed sample reveal the formation of ⟨310⟩ and ⟨200⟩ crystalline phase of SnO₂. However, the relative decrease in peak intensity of the 400 °C annealed sample indicates a deterioration of crystalline quality. The atoms at the surface of the as-grown film are energetically less stable and hence are loosely bound with the surface molecules. As the sample is annealed, the loosely bound atoms of the film surface tend to detach from the surface. This may be attributed to the fact that thermodynamically the system tries to lower its overall energy upon annealing, leading to an increase in concentration of free molecules at the surface of the sample. With increase in annealing temperature, the density of such free molecules increases. With time, these free molecules supersaturate and finally condense on the surface to form larger particles. Hence, the increase of grain size in 200 °C annealing temperature, indicates the coalescences of crystal particles. The average crystallite size is calculated by using Scherrer formula given as [25.26],

$$D = 0.9\lambda/(\beta\cos\theta) \quad (6)$$

where λ is the wavelength of X-ray radiation used and β is the full-width-at-half-maximum (FWHM) of the peaks at the diffracting angle, θ . The micro-strain (ε) of the grown samples is calculated by using the formula given as,

$$\varepsilon = (\beta\cos\theta)/4 \quad (7)$$

The parameters extracted from X-ray diffraction patterns are summarized in Table 1. The lattice strain is measured to decrease with the increase of crystallite size and it becomes 7×10^{-4} for ⟨310⟩ plane of the 200 °C annealed sample having a maximum grain size of ~ 97 nm. This

may be due to the decrease of lattice mismatch between the grains upon annealing.

3.2 Optical characterization of SnO₂/p-Si heterojunction diodes

To investigate the impact of annealing temperature on optical properties of the CBD grown SnO₂ films, spectroscopic ellipsometric (SE) measurement has been performed in the wavelength range of 250–800 nm. The plots of relative amplitude change (ψ) and phase change (Δ) of the as-grown and annealed samples are shown in Fig. 4a–c, respectively. Moreover, to extract the optical constants including absorption coefficient (Tompkins and Hilfiker 2015) and band gap of such films, the results are simulated to fit the experimental data and the relevant model structure has been considered to be air/SnO₂/Si. The optical constants of air and the wavelength of incident light have been considered to remain constant in the fitting process. The modelled values of ψ and Δ for both the as-grown and annealed samples are also plotted in Fig. 4.

It is apparent from such plots that the best-fit data match well with the measured data, thereby, suggesting the model to be extensive over a wide range of wavelength. The band-gap of the as-grown and annealed samples has been found from Tauc's relationship (Viezbicke et al. 2015) as shown in Fig. 5a. The energy band-gap value is found to be 3.0 eV for the as-grown, 200 °C and 400 °C annealed samples (Baco et al. 2012; Igwe and Ugwu 2010). The variation of absorption coefficient (measured from SE data) and grain size (measured from XRD data) with annealing temperature is plotted in Fig. 5b. The absorption coefficient is observed to increase with annealing temperature and is maximum for the 200 °C annealed sample. The nature of variation is similar to the grain size of the dominant [310] plane as obtained from XRD results.

3.3 Electrical characterization of the SnO₂/p-Si heterojunction diodes

The electrical characterization of the SnO₂/p-Si heterojunction diodes is performed by measuring its current density–voltage (J–V) characteristics under both the dark and illuminated condition and the results are plotted in Fig. 6a.

The variation of photocurrent density with applied voltage is highlighted in Fig. 6b. The comparative plots of photocurrent and dark current for different annealing temperatures are shown in Fig. 6c. The maximum photocurrent density of 5.41 mA/cm² with a photo-to-dark current ratio of 3826.7 at zero bias has been obtained for the 200 °C annealed sample.

The plot of variation of short circuit current density and open circuit voltage for different annealing temperatures

Table 1 Summary of the parameters extracted from X-ray diffraction analysis

Sample	Peak position (2θ)	FWHM (2θ)	Crystallite size (nm)	Micro-strain
As-grown	61.8 [310]	0.20	48.37	15×10^{-4}
	37.7 [200]	0.22	39.85	28×10^{-4}
200 °C annealed	61.8 [310]	0.10	96.73	7×10^{-4}
	37.7 [200]	0.20	43.86	25×10^{-4}
400 °C annealed	61.8 [310]	0.11	87.94	8×10^{-4}
	37.6 [200]	0.12	73.0	15×10^{-4}

Fig. 4 Plot of Psi (ψ) and Delta (Δ), for the **a** as-grown; **b** 200 °C annealed; and **c** 400 °C annealed samples, in the wavelength range of 250–800 nm. Solid lines correspond to the experimental data and dotted lines correspond to the simulated data

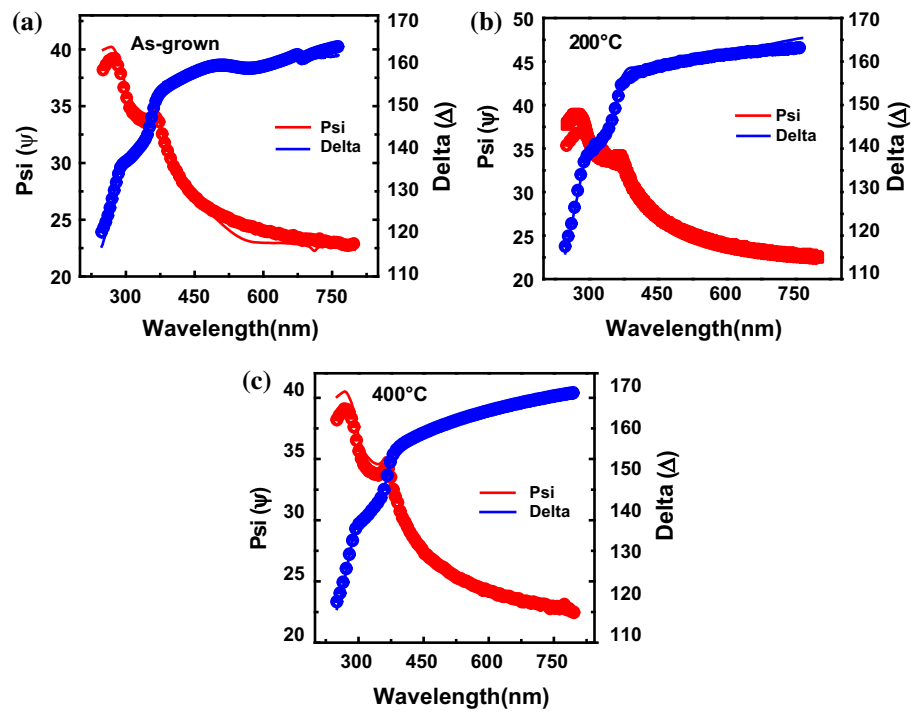
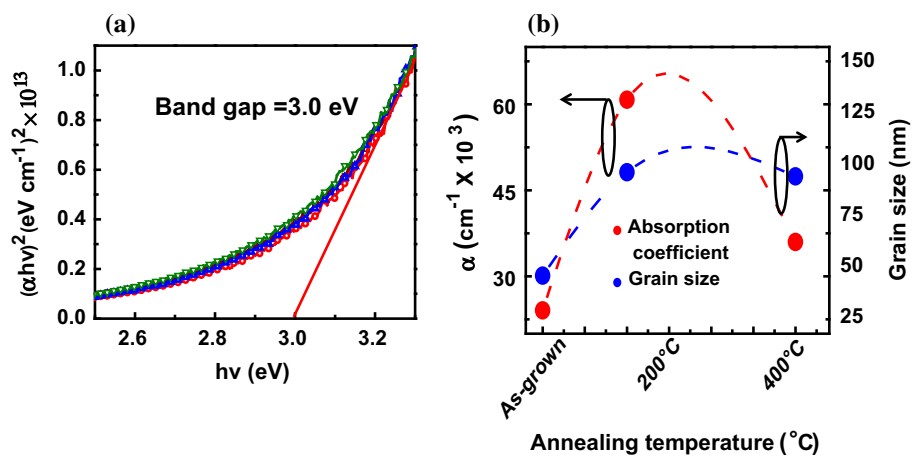


Fig. 5 **a** Tauc’s plot to determine the energy band-gap and; **b** dependence of absorption coefficient and grain size with annealing temperature variation

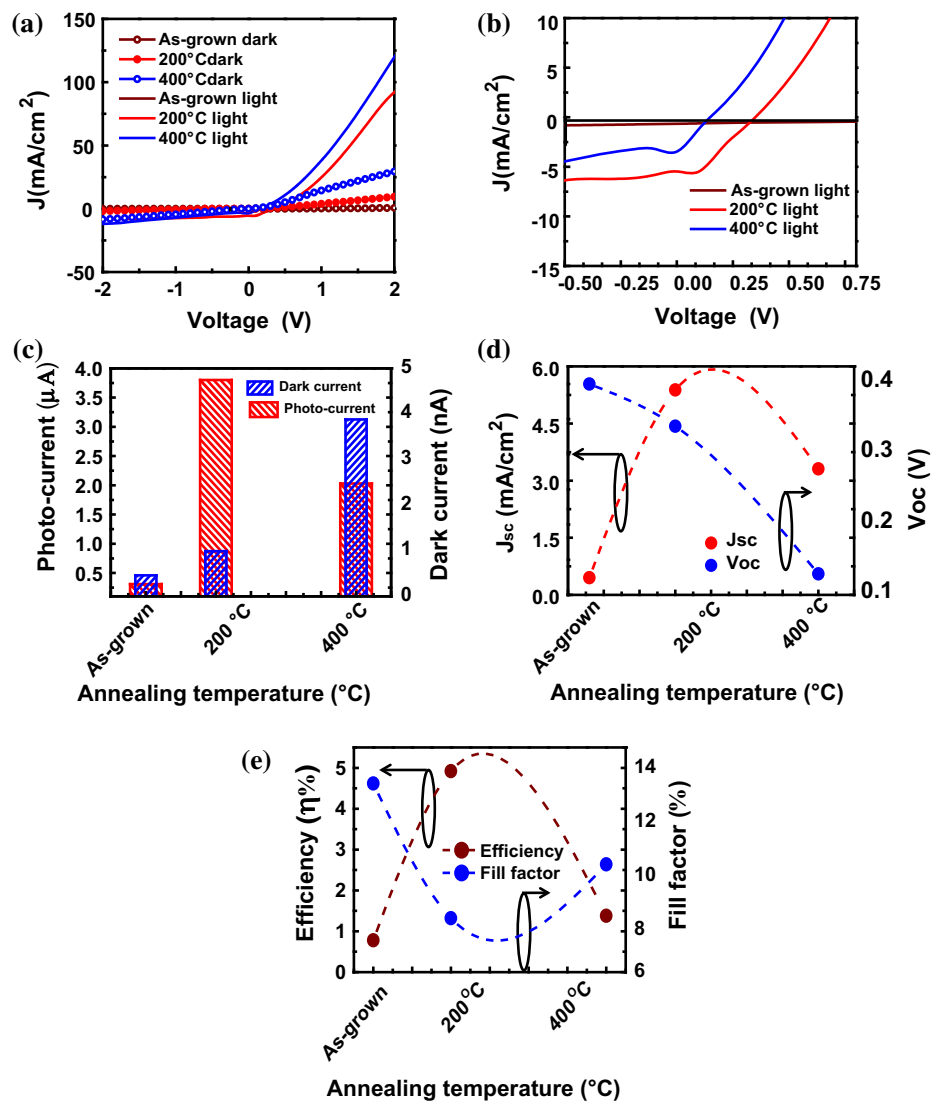


are shown in Fig. 6d. The maximum J_{sc} of 5.41 mA/cm^2 is obtained for the 200 °C annealed sample and the maximum V_{oc} of 0.4 V is obtained for the as-grown sample.

The variation of power conversion efficiency and fill-factor with annealing temperature is shown in Fig. 6e

which suggests the 200 °C annealed film to be appropriate for the best photovoltaic performance among all other samples considered in the current work with an efficiency of 4.9%. The comparative values of short-circuit current density (J_{sc}), open-circuit voltage (V_{oc}), fill factor, Photo-

Fig. 6 **a** Plots of J – V characteristics under dark and illuminated condition; **b** highlighted photo current density at 4th quadrant; **c** photo and dark current variation at zero bias with annealing temperature; **d** The variation of short circuit current density (J_{sc}) and open circuit voltage (V_{oc}) with annealing temperature; **e** Variation of power conversion efficiency and fill-factor with annealing temperature



to-dark current ratio and power conversion efficiency (η) with annealing temperature of the $\text{SnO}_2/\text{p-Si}$ heterojunction diode are summarized in Table 2.

4 Conclusion

SnO_2 thin film has been grown on p-Si substrate by CBD method and annealed in argon (Ar) environment for 10 min at 200 and 400 °C. Morphology, crystalline quality and

optoelectronic properties of the grown SnO_2 thin films have been systematically studied with annealing temperature. It is observed that the annealing temperature has significant impact on controlling the crystallite quality and size of SnO_2 thin films. The largest crystallite size (~ 97 nm) has been measured for 200 °C annealed film. The crystalline nature and optical properties of the film are determined by XRD and SE analyses. The band gap of the grown SnO_2 thin film is obtained to be 3.0 eV and the $\text{SnO}_2/\text{p-Si}$ heterojunction shows a promising photo-to-dark current ratio of

Table 2 The comparative values of short-circuit current density (J_{sc}), open-circuit voltage (V_{oc}), fill-factor, photo-to-dark current ratio at zero bias and power conversion efficiency (η) with annealing temperature

Sample/parameters	As-grown	200 °C	400 °C
J_{sc} (mA/cm ²)	0.45	5.41	3.31
V_{oc} (V)	0.40	0.34	0.13
Fill-factor (%)	13	8	10
Photo-to-dark current ratio at zero bias	683.3	3826.7	530.6
Efficiency (%)	0.78	4.9	1.4

3826.7. Solar cell parameters including short circuit current, open circuit voltage and fill-factor (%) are measured to be 5.41 mA/cm², 0.34 V and 8, respectively, which yields an energy conversion efficiency of 4.9% for the 200 °C annealed sample. Thus, annealing the CBD grown thin film of SnO₂ at 200 °C under Ar environment has been found to be a promising low-cost alternative technological route for the development of solar cell with superior performance.

Acknowledgements Miss. Anannya Bhattacharya and Jenifar Sultana would like to acknowledge the DST inspire program India, for providing financial support to pursue their research. Subhrajit Sikdar and Rajib Saha would like to thank the University Grants Commission and WBDITE for funding their fellowships. The authors would also like to acknowledge the DST Purse program and Center of Excellence (COE), TEQIP and WBDITE for providing infrastructure and financial support to conduct this work.

References

- Baby TT, Ramaprabhu S (2012) Experimental study on the field emission properties of metal oxide nanoparticle-decorated graphene. *J Appl Phys* 111(1–5):034311. <https://doi.org/10.1063/1.3681376>
- Baco S, Chik A, Yassin MdF (2012) Study on optical properties of tin oxide thin film at different annealing temperature. *J Sci Technol* 4:61–71
- Bae S-D, Kwon S-H, Jeong H-S et al (2017) Demonstration of high-performance p-type tin oxide thin film transistors using argon-plasma surface treatments. *Semicond Sci Technol* 32(1–7):075006. <https://doi.org/10.1088/1361-6641/aa72b8>
- Bendjedidi H, Attaf A, Saidi H et al (2015) Properties of n type SnO₂ semiconductor prepared by spray ultrasonic technique for photovoltaic applications. *J Semicond* 36(1–4):123002
- Block T, Schmücker M (2016) Metal oxides for thermochemical energy storage: a comparison of several metal oxide systems. *Sol Energy* 126:195–207. <https://doi.org/10.1016/j.solener.2015.12.032>
- Chen Z, Lai JKL, Shek CH et al (2003) Synthesis and structural characterization of rutile SnO₂ nanocrystals. *J Mater Res* 18:1289–1292. <https://doi.org/10.1557/JMR.2003.0176>
- Cheng HE, Tian DC, Huang KC (2012) Properties of SnO₂ films grown by atomic layer deposition. *Proced Eng* 36:510–515. <https://doi.org/10.1016/j.proeng.2012.03.074>
- Comini E, Faglia G, Sberveglieri G et al (2002) Stable and highly sensitive gas sensors based on semiconducting oxide nanobelts. *Appl Phys Lett* 10:1869–1871. <https://doi.org/10.1063/1.1504867@apl.2019.APLCLASS2019.issue-1>
- Dong Q, Shi Y, Wang K et al (2015) Insight into perovskite solar cells based on SnO₂ compact electron selective layer. *J Phys Chem* 119:10212–10217. <https://doi.org/10.1021/acs.jpcc.5b00541>
- Igwe HU, Ugwu EI (2010) Optical characteristics of nanocrystalline thermal annealed tin oxide (SnO₂) thin film samples prepared by chemical bath deposition technique. *J Adv Appl Sci Res* 1:240–246
- Jadsadapattarakul D, Euvananont C, Thanachayanont C et al (2008) Tin oxide thin films deposited by ultrasonic spray pyrolysis. *Ceram Int* 34:1051–1054. <https://doi.org/10.1016/j.ceramint.2007.09.096>
- Jian Z, Hejing W (2003) The physical meanings of 5 basic parameters for an X-ray diffraction peak and their application. *Chin J Geochem* 22:38–44. <https://doi.org/10.1007/BF02831544>
- Leng D, Wu L, Jiang H, Zhao Y et al (2012) Preparation and properties of SnO₂ film deposited by magnetron sputtering. *Int J Photoenergy* 2012:1–6. <https://doi.org/10.1155/2012/235971>
- Liu Q, Qin MC, Ke WJ et al (2016) Enhanced stability of perovskite solar cells with low-temperature hydrothermally grown SnO₂ electron transport layers. *Adv Funct Mater* 26:6069–6075. <https://doi.org/10.1002/adfm.201600910>
- Mane RS, Lokhande CD (2000) Chemical deposition method for metal chalcogenide thin films. *Mater Chem Phys* 65:1–31. [https://doi.org/10.1016/S0254-0584\(00\)00217-0](https://doi.org/10.1016/S0254-0584(00)00217-0)
- Mun H, Yang H, Park J et al (2015) High electron mobility in epitaxial SnO_{2-x} in semiconducting regime. *APL Mater* 3(1–7):076107. <https://doi.org/10.1063/1.4927470>
- Muniz FTL, Miranda MAR, Santos CM et al (2016) The Scherrer equation and the dynamical theory of X-ray diffraction. *Acta Crystallogr Sect A Found Adv* 72:385–390. <https://doi.org/10.1107/S205327331600365X>
- Patel P, Karmakar A, Jariwala C et al (2013) Preparation and characterization of SnO₂ thin film coating using rf-plasma enhanced reactive thermal evaporation. *Proced Eng* 51:473–479. <https://doi.org/10.1016/j.proeng.2013.01.067>
- Pawar SM, Pawar BS, Kim JH et al (2011) Recent status of chemical bath deposited metal chalcogenide and metal oxide thin films. *Curr Appl Phys* 11:117–161. <https://doi.org/10.1016/j.cap.2010.07.007>
- Pérez-Tomás A, Mingorance A, Tanenbaum D et al (2017) Metal oxides in photovoltaics: all oxide, ferroic, and perovskite solar cells. The future of semiconductor oxides in next-generation solar cells. Elsevier, New York, pp 267–356. <https://doi.org/10.1016/B978-0-12-811165-9.00008-9>
- Rasheed RT, Algae S (2016) Annealing effect of SnO₂ nanoparticles prepared by the sol–gel method. *J Adv Phys* 5:236–240. <https://doi.org/10.1166/jap.2016.1262>
- Sultana J, Paul S, Karmakar A et al (2018) Optimizing the thermal annealing temperature: technological route for tuning the photo-detecting property of p-CuO thin films grown by chemical bath deposition method. *J Mater Sci: Mater Electron* 29:12878–12887. <https://doi.org/10.1007/s10854-018-9407-3>
- Tazikeh S, Akbari A, Talebi A et al (2014) Synthesis and characterization of tin oxide nanoparticles via the co-precipitation method. *Mater Sci Pol* 32:98–101. <https://doi.org/10.2478/s13536-013-0164-y>
- Tompkins HG, Hilfiker JN (2015) Spectroscopic ellipsometry. Practical application to thin film characterization. Momentum Press, New York
- Tripathy SK, Hota BP, Rajeswari PV (2013) Study of optical characteristics of tin oxide thin film prepared by sol–gel method. *Bull Mater Sci* 36:1231–1237. <https://doi.org/10.1007/s12034-013-0582-9>
- Viezbicke BD, Patel S, Davis BE et al (2015) Evaluation of the Tauc method for optical absorption edge determination: ZnO thin films as a model system. *Phys Status Sol (B)* 252:1700–1710. <https://doi.org/10.1002/pssb.201552007>
- Wongsaprom K, Bornphotsawatkun R-a, Swatsitang E (2014) Synthesis and characterization of tin oxide (SnO₂) nanocrystalline powders by a simple modified sol–gel route. *Appl Phys A* 114:373–379. <https://doi.org/10.1007/s00339-013-8197-y>

- Xiong L, Guo Y, Wen J et al (2018) Review on the application of SnO₂ in perovskite solar cells. *Adv Funct Mater* 28(118):1802757. <https://doi.org/10.1002/adfm.201802757>
- Yu X, Marks TJ, Facchetti A (2016) Metal oxides for optoelectronic applications. *Nat Mater* 15:383–396. <https://doi.org/10.1038/nmat4599>
- Zhou L, Xiao L, Yang H et al (2018) Greatly enhanced photovoltaic performance of crystalline silicon solar cells using metal oxide layers by band-gap alignment engineering. *Nanomaterials*. <https://doi.org/10.20944/preprints201804.0353.v1>

Publisher's Note Springer Nature remains neutral with regard to jurisdictional claims in published maps and institutional affiliations.